Oblique QR Decomposition Based Block Partition Strategy for Block Landweber Scheme

Caifang Wang, Cong Che, and Xiaobin Xia

***Abstract*—Block Landweber scheme plays an important role in linear image reconstruction field. In this paper, we propose a block partition strategy based on oblique QR decomposition so as to improve the computational efficiency of block Landweber scheme. And then we provide sensitivity analysis of subproblem from the linear imaging system. Furthermore, in order to prevent excessive memory usage in the process of oblique QR decomposition, we design pseudo code to update these two partition criteria. Finally, we test the performance of our strategy by the image reconstruction of block simultaneous algebra reconstruction technique which is a well known special case of Landweber scheme. Compared with sequential partition, our block partition strategy provides reconstructed images with smaller root mean square errors, but with fewer iteration cycles.**

***Index Terms*—Linear imaging system, QR decomposition, block partition, block Landweber scheme, computational efficiency.**

I. Introduction

WITH the development of medical diagnosis, there are growing concerns about the medical imaging methods. An important model of modern medical imaging is the linear imaging model. However, the imaging matrix in linear imaging model is large and sparse, and its corresponding inverse problem is often ill-posed. Therefore, many researchers have shifted their attention to the design of reconstruction algorithms, regularization methods and the acceleration of reconstruction algorithms in order to get high quality reconstructed images.

There are a number of classical iterative methods used to solve the linear image reconstruction problem. The Kaczmarz method, also known as the algebra reconstruction technique (ART), is an effective iteration algorithm for solving overdetermined systems of linear equations [1]. The traditional Kaczmarz method has a fixed order of iterations, which follows the linear system perse. To accelerate the convergence speed of the Kaczmarz algorithm, many scholars have studied the block partition method and the order of iterations [2], [3], [4], [5], [6]. Some other classical iterative methods such as symmetric successive overrelaxation method (SSOR) and conjugate gradient (CG) method can be used to solve the linear equations with square coefficient matrix. Their preconditioned methods were also studied to improve the efficiency [7], [8]. Moreover, to solve the ill-posed inverse problems, minimizing residual ULT method was established by applying minimizing residual technique to a series of upper and lower triangular methods[9]. In addition, the Landweber scheme can partially deal with the ill-posedness of the problem. It is a general form of a series widely used iterative algorithms [10], covering simultaneous algebra reconstruction technique (SART) [11], Cimmino's method [12], the component averaging (CAV) algorithm [13] and diagonal weighting (DWE) algorithm [14], and so on. The image sequence generated by Landweber scheme converges to a weighted least squares solution of the linear system if the relaxation coefficients are chosen properly [10], [15], [16], [17], but semi-convergence may occur due to the noise of the observed data and the inconsistency of linear equations. To tackle this problem, the stopping rules were involved in [18], [19], [20].

In a sense, the acceleration of reconstruction algorithm is one of the key factors for better application of the algorithm to the actual imaging system. In [10], the authors emphasize that careful selection of the block partitions and the relaxation coefficients can generate high-quality reconstructions with improved computational efficiency. The appropriate relaxation coefficients not only ensure the convergence of the algorithm, but also improve the convergence speed of the algorithm. To achieve faster convergence, some researchers proposed symmetric block iteration based on the symmetric structure of the projection line [21] and some researchers used a strategy of partition the imaging matrix according to the projection angle [22]. To find the optimal relaxation coefficients, a matlab package was designed in 2011 [23]. Different from the matlab package, new relaxation strategies and new weighting matrix were proposed to accelerate the convergence of the iteration [24]. In term of computational efficiency improvement, block iteration is a useful technique. In [25], the authors defined column correlations of the matrix transformed from QR decomposition of the imaging matrix and applied the block partition method based on column correlations to Kaczmarz method. Similarly, for Landweber scheme, the fixed block-iteration and variable block-iteration were introduced utilized [26], [27].

In order to improve the computational efficiency of the block iterative method, in this paper we also study the block partition method of imaging matrix from the perspective of well-posedness of submatrices. A weighted relative volume method is to better solve the linear imaging problem. The relative volume method was widely used in surveying and mapping science [28]. To make this method more applicable to weighted least squares problem, we desire weighted relative volume criterion for block partition. To stabilize block partition results, the weighted column correlation is used as an auxiliary criterion. Different from the cases in surveying and mapping science, the system matrix in imaging problem is huge and it is difficult to directly calculate and store the

Manuscript received January 11, 2023; revised June 2, 2023. This work was supported in part by Shanghai University Science and Technology Innovation Action Plan Local University Capacity Building Project (23010502100).

C. Wang is a professor of College of Sciences, Shanghai Maritime University, Shanghai, 201036 P. R. China (email: cfwang@shmtu.edu.cn).

C. Che is a graduate student of College of Sciences, Shanghai Maritime University, Shanghai, 201036 P. R. China (email: 1033440295@qq.com).

X. Xia is a graduate student of College of Sciences, Shanghai Maritime University, Shanghai, 201036 P. R. China (email: xxb3075099807@163.com).

results of oblique QR decomposition in RAM. Therefore, we also design pseudo codes where the R matrix is directly used to update partition strategy while the Q matrix is not stored. Finally, numerical experiments are conducted to test the performance of our block partition strategy.

The rest of the paper is organized as follows. Section II induces the linear imaging problem as well as the Landweber scheme. In Section III, we describe the details of block partition strategy based on oblique QR decomposition and then provide the concrete realization of the strategy. Then we validate the performances of the block partition strategy by the numerical tests of block Landweber scheme in Section IV. Some related issues are also discussed in this section. Finally, the conclusion is presented in Section V.

II. Linear image reconstruction problem and block Landweber scheme

A linear imaging system in real space can be modeled as

$$\boldsymbol{A}\boldsymbol{x} = \boldsymbol{b}, \tag{1}$$

where $\boldsymbol{A} \in \mathbb{R}^{m\times n}$ is the imaging matrix, $\boldsymbol{b} \in \mathbb{R}^m$ is the measurement data, and $\boldsymbol{x} \in \mathbb{R}^n$ is the unknown image to be reconstructed.

In consideration of the ill-posedness of the problem and noisy observed data $\boldsymbol{b}$, the solution of the linear imaging problem is usually found through the following weighted least squares problem

$$\min_{\boldsymbol{x}\in\mathbb{R}^n_{\boldsymbol{V}}} \quad L_{\boldsymbol{W}}(\boldsymbol{x}) = \frac{1}{2}\|\boldsymbol{A}\boldsymbol{x} - \boldsymbol{b}\|^2_{\boldsymbol{W}}. \tag{2}$$

Here $\boldsymbol{W}$ and $\boldsymbol{V}$ are two positive definite diagonal matrices of orders m and n, respectively. The weighted norm $\|\cdot\|_{\boldsymbol{V}}$ and weighted inner product $\langle\cdot,\cdot\rangle_{\boldsymbol{V}}$ in $\mathbb{R}^n$ are defined as follows

$$\|\boldsymbol{x}\|_{\boldsymbol{V}} = \sqrt{\langle\boldsymbol{x},\boldsymbol{x}\rangle_{\boldsymbol{V}}}, \quad \langle\boldsymbol{x},\boldsymbol{x}\rangle_{\boldsymbol{V}} = \langle\boldsymbol{V}\boldsymbol{x},\boldsymbol{x}\rangle, \quad \forall\boldsymbol{x}\in\mathbb{R}^n. \tag{3}$$

The weighted inner product $\langle\cdot,\cdot\rangle_{\boldsymbol{W}}$ and weighted norm $\|\cdot\|_{\boldsymbol{W}}$ can be defined similarly.

The Landweber scheme is a widely used method to solve the linear imaging problem. Its iteration formula is

$$\boldsymbol{x}^{(k+1)} = \boldsymbol{x}^{(k)} + \lambda_k\boldsymbol{V}^{-1}\boldsymbol{A}^{\mathrm{T}}\boldsymbol{W}(\boldsymbol{b} - \boldsymbol{A}\boldsymbol{x}^{(k)}), \quad k = 1,2,\ldots \tag{4}$$

where $\lambda_k > 0$ is the relaxation coefficient. A block version of Landweber scheme can be used so as to improve computational efficiency. Assume that B_t $(t = 1,2,\ldots,T)$ is a nonempty subset partitioned from the index set $\{1,2,\cdots,m\}$ and each of B_t consists of $m_t \geq 1$ indices. Let $\boldsymbol{A}_t \in \mathbb{R}^{m_t\times n}$, $\boldsymbol{b}_t \in \mathbb{R}^{m_t}$ and $\boldsymbol{W}_t \in \mathbb{R}^{m_t\times m_t}$ be the corresponding blocks from $\boldsymbol{A}$, $\boldsymbol{b}$ and $\boldsymbol{W}$ with respect to the partition B_t. Then the block version of the Landweber scheme can be written as

$$\boldsymbol{x}^{(kT+t+1)} = \boldsymbol{x}^{(kT+t)} + \lambda_{kT+t}\boldsymbol{V}^{-1}(\boldsymbol{A}_t)^{\mathrm{T}}\boldsymbol{W}_t(\boldsymbol{b}_t - \boldsymbol{A}_t\boldsymbol{x}^{(kT+t)}), \quad t = 1,2,\ldots,T. \tag{5}$$

III. Block partition strategy base on oblique QR decomposition

In this section, we propose a partition strategy based on thin oblique QR decomposition with respect to weighted norm, and then provide the concrete realization of the strategy.

A. Block Partition Strategy

Assume that the tth block $\boldsymbol{A}_t^{\mathrm{T}}$ contains s vectors and its thin oblique QR decomposition $\boldsymbol{A}_t^{\mathrm{T}} = \boldsymbol{Q}_t\boldsymbol{R}_t$ is with the form

$$(\boldsymbol{a}_{i_1^t}^{\mathrm{T}},\cdots,\boldsymbol{a}_{i_s^t}^{\mathrm{T}}) = (\boldsymbol{q}_{i_1^t},\cdots,\boldsymbol{q}_{i_s^t})\begin{bmatrix} r_{i_{11}^t} & \cdots & r_{i_{1s}^t} \\ & \ddots & \vdots \\ & & r_{i_{ss}^t} \end{bmatrix}, \tag{6}$$

where

$$\langle\boldsymbol{q}_{i_k^t},\boldsymbol{q}_{i_j^t}\rangle_{\boldsymbol{V}_t^{-1}} = \begin{cases} 0, & k\neq j, \\ 1, & k = j. \end{cases} \tag{7}$$

For a new vector $\boldsymbol{a}_{i_{s+1}^t}$, we calculate new thin QR decomposition

$$(\boldsymbol{A}_t^{\mathrm{T}}, \boldsymbol{a}_{i_{s+1}^t}^{\mathrm{T}}) = (\boldsymbol{Q}_t, \boldsymbol{q}_{i_{s+1}^t})\widetilde{\boldsymbol{R}}_t. \tag{8}$$

Let $\widetilde{\boldsymbol{R}}_t = (\boldsymbol{r}_1,\cdots,\boldsymbol{r}_s,\boldsymbol{r}_{s+1})$. Given two predetermined thresholds κ_1 and κ_2, once

$$\frac{\max\limits_{1\leq k\leq s+1}\{r_{i_{kk}^t}\}}{\min\limits_{1\leq k\leq s+1}\{r_{i_{kk}^t}\}} \leq \kappa_1 \quad \text{and} \quad \frac{\prod\limits_{k=1}^{s+1}\|\boldsymbol{r}_k\|_{\widetilde{\boldsymbol{W}}_t}}{\sqrt{\det(\widetilde{\boldsymbol{R}}_t^{\mathrm{T}}\widetilde{\boldsymbol{W}}_t\widetilde{\boldsymbol{R}}_t)}} \leq \kappa_2, \tag{9}$$

then $\boldsymbol{a}_{i_{s+1}^t}^{\mathrm{T}}$ can be added to $\boldsymbol{A}_t^{\mathrm{T}}$.

Remark III.1. *1. The former criterion in (9) represents the weighted column correlation of* $(\boldsymbol{A}_t^{\mathrm{T}}, \boldsymbol{a}_{i_{s+1}^t}^{\mathrm{T}})$.

2. The latter criterion in (9) is the weighted relative volume:

1) $\sqrt{\det(\widetilde{\boldsymbol{R}}_t^{\mathrm{T}}\widetilde{\boldsymbol{W}}_t\widetilde{\boldsymbol{R}}_t)}$ *represent the volume of the hyper-parallel polyhedron composed by the non-zero column vectors of* $\widetilde{\boldsymbol{R}}_t^{\mathrm{T}}$ *w.r.t.* $\widetilde{\boldsymbol{W}}_t$*-norm.*
2) $\prod_{i=1}^{s+1}\|\boldsymbol{r}_i\|_{\widetilde{\boldsymbol{W}}_t}$ *represents the maximum volume of a hyper-parallel polyhedron that is formed by the same set of column vectors after changing azimuth.*

Proposition III.2. *Let* $\bar{\boldsymbol{A}}_t = \boldsymbol{W}_t^{\frac{1}{2}}\boldsymbol{A}_t\boldsymbol{V}^{-\frac{1}{2}}$*. Consider the thin QR decomposition of* $\bar{\boldsymbol{A}}_t^{\mathrm{T}}$ *and thin oblique QR decomposition of* $\boldsymbol{A}_t^{\mathrm{T}}$

$$\bar{\boldsymbol{A}}_t^{\mathrm{T}} = \bar{\boldsymbol{Q}}_t\bar{\boldsymbol{R}}_t, \qquad \boldsymbol{A}_t^{\mathrm{T}} = \boldsymbol{Q}_t\boldsymbol{R}_t. \tag{10}$$

Then

1) $\langle\bar{\boldsymbol{q}}_{i_k^t},\bar{\boldsymbol{q}}_{i_j^t}\rangle = \langle\boldsymbol{q}_{i_k^t},\boldsymbol{q}_{i_j^t}\rangle_{\boldsymbol{V}^{-1}}$.
2) $\bar{\boldsymbol{R}}_t^{\mathrm{T}} = \boldsymbol{W}_t^{\frac{1}{2}}\boldsymbol{R}_t^{\mathrm{T}}$.

Proof: By simple calculation, we have

$$\bar{\boldsymbol{Q}}_t\bar{\boldsymbol{R}}_t = \bar{\boldsymbol{A}}_t^{\mathrm{T}} = \boldsymbol{V}^{-\frac{1}{2}}\boldsymbol{A}_t^{\mathrm{T}}\boldsymbol{W}_t^{-\frac{1}{2}} = \boldsymbol{V}^{-\frac{1}{2}}\boldsymbol{Q}_t\boldsymbol{R}_t\boldsymbol{W}_t^{-\frac{1}{2}}. \tag{11}$$

Let $\bar{\boldsymbol{R}}_t = \boldsymbol{R}_t\boldsymbol{W}_t^{\frac{1}{2}}$ and $\bar{\boldsymbol{Q}}_t = \boldsymbol{V}^{-\frac{1}{2}}\boldsymbol{Q}_t$. Using the column block form of $\bar{\boldsymbol{Q}}_t$ and $\boldsymbol{Q}_t$, we have

$$\begin{aligned}\langle\bar{\boldsymbol{q}}_{i_k^t},\bar{\boldsymbol{q}}_{i_j^t}\rangle &= \langle\boldsymbol{V}^{-\frac{1}{2}}\boldsymbol{q}_{i_k^t},\boldsymbol{V}^{-\frac{1}{2}}\boldsymbol{q}_{i_j^t}\rangle \\ &= \langle\boldsymbol{V}^{-1}\boldsymbol{q}_{i_k^t},\boldsymbol{q}_{i_j^t}\rangle = \langle\boldsymbol{q}_{i_k^t},\boldsymbol{q}_{i_j^t}\rangle_{\boldsymbol{V}^{-1}}.\end{aligned} \tag{12}$$

■

B. Sensitivity Analysis

Applying thin oblique QR decomposition to the tth subproblem, the linear equations can be written as

$$\boldsymbol{R}_t^{\mathrm{T}}\boldsymbol{y}_t = \boldsymbol{b}_t, \tag{13}$$

where $\boldsymbol{y}_t = \boldsymbol{Q}_t^{\mathrm{T}}\boldsymbol{x}_t$. In the following, we analyze the sensitivity of above equation.

Theorem III.3. *Let* $\boldsymbol{F}_t = (\boldsymbol{F}_1^{\mathrm{T}}, \cdots, \boldsymbol{F}_s^{\mathrm{T}})^{\mathrm{T}} \in \mathbb{R}^{s\times s}$, $\boldsymbol{b}_t^\delta = (\boldsymbol{b}_1^\delta, \cdots, \boldsymbol{b}_s^\delta)^{\mathrm{T}} \in \mathbb{R}^s$. *From the parameterized system*

$$(\boldsymbol{R}_t^{\mathrm{T}} + \varepsilon\boldsymbol{F}_t)\boldsymbol{y}_t(\varepsilon) = \boldsymbol{b}_t + \varepsilon\boldsymbol{b}_t^\delta, \quad \boldsymbol{y}_t(0) = \boldsymbol{y}_t, \tag{14}$$

it can be deduced that

$$\frac{\|\boldsymbol{y}_t(\varepsilon) - \boldsymbol{y}_t\|_2}{\|\boldsymbol{y}_t\|_2} \le \varepsilon\kappa_1\left(\frac{\|\boldsymbol{b}_t^\delta\|_2}{\|\boldsymbol{b}_t\|_2} + \frac{\|\boldsymbol{F}_t\|_2}{\|\boldsymbol{R}_t^{\mathrm{T}}\|_2}\right) + O(\varepsilon^2), \tag{15}$$

and

$$\frac{\|\boldsymbol{y}_t(\varepsilon)-\boldsymbol{y}_t\|_{\boldsymbol{W}_t^{-1}}}{\|\boldsymbol{y}_t\|_{\boldsymbol{W}_t^{-1}}} \le \varepsilon\kappa_2\sum_{i=1}^{s}\left(\frac{|\boldsymbol{b}_i^\delta|}{|\boldsymbol{b}_{t_i}|} + \frac{\|\boldsymbol{F}_i\|_{\boldsymbol{W}_t}}{\|\boldsymbol{r}_i\|_{\boldsymbol{W}_t}}\right) + O(\varepsilon^2). \tag{16}$$

Proof: 1. The Taylor series expansion for $\boldsymbol{y}_t(\varepsilon)$ has the form

$$\boldsymbol{y}_t(\varepsilon) = \boldsymbol{y}_t + \varepsilon\dot{\boldsymbol{y}}_t(0) + O(\varepsilon^2), \tag{17}$$

where $\dot{\boldsymbol{y}}_t(0) = \boldsymbol{R}_t^{-T}(\boldsymbol{b}_t^\delta - \boldsymbol{F}_t\boldsymbol{y}_t)$. Thus

$$\begin{aligned}\frac{\|\boldsymbol{y}_t(\varepsilon) - \boldsymbol{y}_t\|_2}{\|\boldsymbol{y}_t\|_2} &\le \varepsilon\frac{\|\boldsymbol{R}_t^{-\mathrm{T}}(\boldsymbol{b}_t^\delta - \boldsymbol{F}_t\boldsymbol{y}_t)\|_2\|\boldsymbol{R}_t^T\|_2}{\|\boldsymbol{R}_t^{\mathrm{T}}\|_2\|\boldsymbol{y}_t\|_2} + O(\varepsilon^2)\\ &\le \varepsilon\|\boldsymbol{R}_t^{-\mathrm{T}}\|_2\|\boldsymbol{R}_t^T\|_2\left(\frac{\|\boldsymbol{b}_t^\delta\|_2}{\|\boldsymbol{b}_t\|_2} + \frac{\|\boldsymbol{F}_t\|_2}{\|\boldsymbol{R}_t^T\|_2}\right)\\ &\quad + O(\varepsilon^2).\end{aligned} \tag{18}$$

According to the definition of matrix norm and (9), we get the estimation (15).

2. Let $\boldsymbol{M}^{[i,j]}$ be a matrix obtained from $\boldsymbol{M}$ by deleting the ith row and jth column of $\boldsymbol{M}$, and $\boldsymbol{M}^{[i,\cdot]}$ be a matrix obtained from $\boldsymbol{M}$ by deleting the ith row of $\boldsymbol{M}$.

According to Cauchy-Binet Theorem and Hadamard inequality, we have

$$\begin{aligned}&\sum_{j=1}^{s}\det((\boldsymbol{R}_t^{\mathrm{T}}\boldsymbol{W}_t^{\frac{1}{2}})^{[i,j]})\det((\boldsymbol{R}_t^{\mathrm{T}}\boldsymbol{W}_t^{\frac{1}{2}})^{[i,k]})\\ =\ &\det((\boldsymbol{R}_t^{\mathrm{T}}\boldsymbol{W}_t^{\frac{1}{2}})^{[i,\cdot]}(\boldsymbol{W}_t^{\frac{1}{2}}\boldsymbol{R})_t^{[\cdot,k]})\\ \le\ &\frac{\prod_{j=1}^{s}\|\boldsymbol{W}_t^{\frac{1}{2}}\boldsymbol{r}_j\|^2}{\|\boldsymbol{W}_t^{\frac{1}{2}}\boldsymbol{r}_i\|\ \|\boldsymbol{W}_t^{\frac{1}{2}}\boldsymbol{r}_k\|} = \frac{\prod_{j=1}^{s}\|\boldsymbol{r}_j\|_{\boldsymbol{W}_t}^2}{\|\boldsymbol{r}_i\|_{\boldsymbol{W}_t}\ \|\boldsymbol{r}_k\|_{\boldsymbol{W}_t}},\end{aligned} \tag{19}$$

for $1 \le i, k \le s$. Using Cramer's Rule, we calculate

$$\begin{aligned}&\|\dot{\boldsymbol{y}}_t(0)\|_{\boldsymbol{W}_t^{-1}}^2 = \sum_{j=1}^{s}(\boldsymbol{W}_t^{-\frac{1}{2}}\dot{\boldsymbol{y}}_t(0))_j^2\\ =\ &\frac{1}{\det(\boldsymbol{R}_t^{\mathrm{T}}\boldsymbol{W}_t\boldsymbol{R}_t)}\sum_{j=1}^{s}\left\{\sum_{i=1}^{s}(-1)^{i+j}(\boldsymbol{b}_i^\delta - \boldsymbol{F}_i\boldsymbol{y}_t)\right.\\ &\left.\det((\boldsymbol{R}_t^{\mathrm{T}}\boldsymbol{W}_t^{\frac{1}{2}})^{[i,j]})\right\}^2\\ =\ &\frac{1}{\det(\boldsymbol{R}_t^{\mathrm{T}}\boldsymbol{W}_t\boldsymbol{R}_t)}\sum_{i=1}^{s}\sum_{k=1}^{s}(-1)^{i+k}\\ &(\boldsymbol{b}_i^\delta - \boldsymbol{F}_i\boldsymbol{y}_t)(\boldsymbol{b}_k^\delta - \boldsymbol{F}_k\boldsymbol{y}_t)\\ &\sum_{j=1}^{s}\det((\boldsymbol{R}_t^{\mathrm{T}}\boldsymbol{W}_t^{\frac{1}{2}})^{[i,j]})\det((\boldsymbol{R}_t^{\mathrm{T}}\boldsymbol{W}_t^{\frac{1}{2}})^{[k,j]})\\ \le\ &\frac{\prod_{j=1}^{s}\|\boldsymbol{r}_j\|_{\boldsymbol{W}_t}^2}{\det(\boldsymbol{R}_t^{\mathrm{T}}\boldsymbol{W}_t\boldsymbol{R}_t)}\left\{\sum_{i=1}^{s}(-1)^i\frac{\boldsymbol{b}_i^\delta - \boldsymbol{F}_i\boldsymbol{y}_t}{\|\boldsymbol{r}_i\|_{\boldsymbol{W}_t}}\right\}^2\\ \le\ &\kappa_2^2\|\boldsymbol{y}_t\|_{\boldsymbol{W}_t^{-1}}^2\left\{\sum_{i=1}^{s}\left(\frac{|\boldsymbol{b}_i^\delta|}{|\boldsymbol{b}_{t_i}|} + \frac{\|\boldsymbol{F}_i\|_{\boldsymbol{W}_t}}{\|\boldsymbol{r}_i\|_{\boldsymbol{W}_t}}\right)\right\}^2.\end{aligned} \tag{20}$$

Combining with (17) and (20), we finally arrive at (16). ■

C. Construction of Upper Triangle Matrix

In image reconstruction problem, the imaging matrix $\boldsymbol{A}$ is large and sparse. But the matrix $\boldsymbol{Q}_t$ is no longer sparse and therefore it is more difficult to store $\boldsymbol{Q}_t$ in RAM. In the following we provide the details of the new block partition strategy without storing matrices $\boldsymbol{A}$ and $\boldsymbol{Q}_t$. We first construct $\boldsymbol{R}_t$ following Gram-Schmidt method.

1) Calculating the first element $r_{i_{11}^t}$ of $\boldsymbol{R}_t$.
Using

$$\begin{cases} r_{i_{11}^t}\boldsymbol{q}_{i_{11}^t} = \boldsymbol{a}_{i_{11}^t}^{\mathrm{T}}, & r_{i_{11}^t} \ge 0,\\ \langle \boldsymbol{q}_{i_{11}^t}, \boldsymbol{q}_{i_{11}^t}\rangle_{\boldsymbol{V}^{-1}} = 1, \end{cases} \tag{21}$$

we have

$$r_{i_{11}^t} = \sqrt{\left\langle \boldsymbol{a}_{i_{11}^t}^{\mathrm{T}}, \boldsymbol{a}_{i_{11}^t}^{\mathrm{T}}\right\rangle_{\boldsymbol{V}^{-1}}}. \tag{22}$$

2) Appending column vector of $\boldsymbol{R}_t$.
Since

$$\boldsymbol{a}_{i_{s+1}^t}^{\mathrm{T}} = \sum_{k=1}^{s} r_{i_{k,s+1}^t}\boldsymbol{q}_{i_k^t} + r_{i_{s+1,s+1}^t}\boldsymbol{q}_{i_{s+1}^t}, \tag{23}$$

then

$$\begin{aligned} r_{i_{1,s+1}^t} &= \left\langle \boldsymbol{q}_{i_1^t}, \boldsymbol{a}_{i_{s+1}^t}^{\mathrm{T}}\right\rangle_{\boldsymbol{V}^{-1}}\\ &= \frac{1}{r_{i_{11}^t}}\left\langle \boldsymbol{a}_{i_1^t}^{\mathrm{T}}, \boldsymbol{a}_{i_{s+1}^t}^{\mathrm{T}}\right\rangle_{\boldsymbol{V}^{-1}}, \end{aligned} \tag{24}$$

and for $k = 2, \ldots, s$

$$\begin{aligned} r_{i_{k,s+1}^t} &= \left\langle \boldsymbol{q}_{i_k^t}, \boldsymbol{a}_{i_{s+1}^t}^{\mathrm{T}}\right\rangle_{\boldsymbol{V}^{-1}}\\ &= \frac{1}{r_{i_{kk}^t}}\left\langle \boldsymbol{a}_{i_k^t}^{\mathrm{T}} - \sum_{l=1}^{k-1} r_{i_{l,k}^t}\boldsymbol{q}_{i_l^t}, \boldsymbol{a}_{i_{s+1}^t}^{\mathrm{T}}\right\rangle_{\boldsymbol{V}^{-1}}\\ &= \frac{1}{r_{i_{kk}^t}}\left(\left\langle \boldsymbol{a}_{i_k^t}^{\mathrm{T}}, \boldsymbol{a}_{i_{s+1}^t}^{\mathrm{T}}\right\rangle_{\boldsymbol{V}^{-1}} - \sum_{l=1}^{k-1} r_{i_{l,k}^t}r_{i_{l,s+1}^t}\right) \end{aligned} \tag{25}$$

Finally, the last element of $\boldsymbol{R}_t$ can be calculated by

$$r^2_{i^t_{s+1},s+1} = \left\langle \boldsymbol{a}^{\mathrm{T}}_{i^t_{s+1}}, \boldsymbol{a}^{\mathrm{T}}_{i^t_{s+1}} \right\rangle_{\boldsymbol{V}^{-1}} - \sum_{l=1}^{s} r^2_{i^t_{l,s+1}}. \quad (26)$$

Next, we introduce an algorithm of updating the upper triangular matrix $\boldsymbol{R}_t$. Suppose $\boldsymbol{R}_t^{\mathrm{T}}$ is stored in a lower triangular structure R and there are s rows in R. The vector to be examined is $\boldsymbol{a}_{i^t_{s+1}}$. Then the $(s+1)$th row of R can be calculated by Algorithm 1.

Algorithm 1 Construction of lower triangular storage structure

Require: The new vector to be checked: $\boldsymbol{a}_{i^t_{s+1}}$
Lower triangular storage structure R with s rows
Ensure: Lower triangular storage structure R with $s+1$ rows

for j from 1 to $s+1$ **do**
  $R[s+1][j] \leftarrow \left\langle \boldsymbol{a}^{\mathrm{T}}_{i^t_{s+1}}, \boldsymbol{a}^{\mathrm{T}}_{i^t_j} \right\rangle_{\boldsymbol{V}^{-1}}$
end for
$R[s+1][1] \leftarrow R[s+1][1]/R[1][1]$
for j from 2 to s **do**
  for l from 1 to $j-1$ **do**
    $R[s+1][j] \leftarrow R[s+1][j] - R[j][l] * R[s+1][l]$
  end for
  $R[s+1][j] \leftarrow R[s+1][j]/R[j][j]$
end for
for l from 1 to s **do**
  $R[s+1][s+1] \leftarrow R[s+1][s+1] - R[s+1][l] * R[s+1][l]$
end for
$R[s+1][s+1] \leftarrow \sqrt{R[s+1][s+1]}$

D. Realization of Block Partition Strategy

Once the lower triangular storage structure is fixed, Algorithm 2 is put to use achieving the row partition of matrix $\boldsymbol{A}$. Let $MaxNum$ be the upper limit of storage elements allowed in each block, κ_1 and κ_2 be predetermined numbers of block partition criteria. The outputs of Algorithm 2 are two long vectors. The first vector $Block$ stores the row indices of different blocks, and the second vector $BlockLength$ stores the number of vectors in each block in turn.

$Block$	$BlockLength$
$B_1 = \{i^1_1, \ldots, i^1_{m_1}\}$	m_1
$\vdots$	$\vdots$
$B_t = \{i^t_1, \ldots, i^t_{m_t}\}$	m_t
$\vdots$	$\vdots$
$B_s = \{i^s_1, \ldots, i^s_{m_s}\}$	m_s

Fig 1. The outputs of Algorithm 2

IV. Numerical tests for block partition and block Landweber scheme

In this section, we study the reconstruction performance of block Landweber scheme with the new partition method introduced above. All the numerical tests are taken on a DELL OptiPlex 9020 desktop with memory 8GB and processor Intel(R) Core(TM) i7-4790 CPU @360GHz (8 CPUs). The operating system is Ubuntu with kernel 3.19.0-93-generic. The compiler is gcc 4.9.2.

Algorithm 2 Block partition method without storing orthogonal matrix

Require: Block partition criterion $\kappa_1,\ \kappa_2$
Maximum number of indices allowed in each block $MaxNum$
Number of rows of system matrix: m
Ensure: A vector of indices sets: $Block$
A vector of the length for each block: $BlockLength$

Initialization of indicator set: $idx = \{1, 2, \ldots, m\}$
$Block,\ BlockLength \leftarrow \varnothing$
while $idx.size() > 0$ **do**
  Get the first element of idx: i^t_1
  $B_t \leftarrow \{i^t_1\}$
  Remove i^t_1 from idx
  $s \leftarrow 1$
  $R[1][1] \leftarrow \sqrt{\left\langle \boldsymbol{a}^{\mathrm{T}}_{i^t_1}, \boldsymbol{a}^{\mathrm{T}}_{i^t_1} \right\rangle_{\boldsymbol{V}^{-1}}}$
  $d,\ r \leftarrow R[1][1] * R[1][1] * W[i^t_1]$
  $d_{\min}, d_{\max} \leftarrow R[1][1]$
  pnt points to the first element of idx
  while pnt dose not point to the end of idx **and** $s < MaxNum$ **do**
    Get the element i^t_{s+1} pointed by pnt and the vector $\boldsymbol{a}_{i^t_{s+1}}$
    pnt points to the next element in idx
    Update R using **Algorithm 1**
    for i from 1 to s **do**
      $r_{temp}[i] \leftarrow r[i] + R[i][s+1] * R[i][s+1] * W[i^t_{s+1}]$
    end for
    if $\frac{\max\{d_{\max}, R[s+1][s+1]\}}{\min\{d_{\min}, R[s+1][s+1]\}} \le \kappa_1$ **and** $\frac{\prod_{i=1}^{s} r_{temp}[i]}{d} \le \kappa_2$ **then**
      Push back i^t_{s+1} to B_t
      Remove i^t_{s+1} from idx
      $d \leftarrow d * R[s+1][s+1] * R[s+1][s+1] * W[i^t_{s+1}]$
      for i from 1 to s **do**
        $r[i] \leftarrow r_{temp}[i]$
      end for
      Push back $R[s+1][s+1] * R[s+1][s+1] * W[i^t_{s+1}]$ to r
      $d_{\max} \leftarrow \max\{d_{\max}, R[s+1][s+1]\}$
      $d_{\min} \leftarrow \min\{d_{\min}, R[s+1][s+1]\}$
      $s \leftarrow s+1$
    else
      Remove last row of R
    end if
  end while
  Push back B_t to $Block$
  Push back s to $BlockLength$
end while

A. Phantom and Parameter Setting

A fan-beam X-ray CT model is used in our numerical experiments. The parameters of the imaging model are listed in Table I.

SART is a well known special case of general Landweber scheme. We use SART to reconstruct the image in the following. The diagonal weighted matrices $\boldsymbol{V}$ and $\boldsymbol{W}$ of

TABLE I
PARAMETER SETTING RELATED TO IMAGING

Imaging model	fan-beam X-ray CT
Detectors	$256 \times 360 \quad (m = 256 \times 360)$
Phantom	low contract Shepp-Logan
Image resolution	$256 \times 256 \quad (n = 256 \times 256)$
a_{ij}	length of the intersection line between the ith ray and the jth pixel

SART are defined as

$$v_j = \boldsymbol{A}_{+,j} = \sum_{i=1}^{m} \mid a_{ij} \mid, \tag{27}$$

$$\frac{1}{w_i} = \boldsymbol{A}_{i,+} = \sum_{j=1}^{n} \mid a_{ij} \mid, \tag{28}$$

where v_j and w_i are the diagonal elements of $\boldsymbol{V}$ and $\boldsymbol{W}$, respectively.

We treat the measurement data obtained from one projection as a whole. That means the row indices corresponding to the same angle in sinogram either enter the block at the same time or not. The parameters of block partition method are set as Table 2. Selecting the first index randomly from 1 to 360 and executing Algorithm 2, we get the output blocks of partition. Next we can apply the partitioned blocks to block version of SART.

TABLE II
PARAMETER SETTING RELATED TO BLOCK PARTITION METHOD

κ_1	5.00
κ_2	σ^s, where $\sigma = 1.03$ is a scale factor and s is the number of row indicators in the current block
$MaxNum$	256×4

Relative residual (RES) and root mean squared error (RMSE) are often used to measure reconstruction efficiency and reconstruction quality. Combining the weighted matrices $\boldsymbol{W}$ and $\boldsymbol{V}$, RES and RMSE are defined as

$$RES = \frac{\|\boldsymbol{b} - \boldsymbol{A}\boldsymbol{x}^{(k)}\|_{\boldsymbol{W}}^2}{\|\boldsymbol{b}\|_{\boldsymbol{W}}^2}, \tag{29}$$

$$RMSE = \frac{1}{\sqrt{n}}\|\boldsymbol{x}^{(k)} - \boldsymbol{x}^*\|_{\boldsymbol{V}}, \tag{30}$$

where $\boldsymbol{x}^{(k)}$ is the reconstructed result of the kth iteration cycle and $\boldsymbol{x}^*$ is the real image.

B. Reconstruction with Sequential Blocks

To test the performance of the block partition method proposed in this paper (QRBlock), we compared other two different partition methods as follows.

- SeqBlock1: $B_t = \{2^{10}(t-1)+1, \ldots, 2^{10}t\}$.
- SeqBlock2: $B_t = \{\sum_{i=1}^{t-1} m_i + 1, \ldots, \sum_{i=1}^{t} m_i\}$.

Assume that the traversal of all blocks is a block iteration cycle, and during one block iteration cycle λ_k is a constant. The iteration process from $\boldsymbol{x}^{(kT)}$ to $\boldsymbol{x}^{((k+1)T)}$ is

$$\boldsymbol{x}^{((k+1)T)} = \prod_{t=T}^{1} \left(\boldsymbol{I} - \lambda_k \boldsymbol{V}^{-1}\boldsymbol{A}_t^{\mathrm{T}}\boldsymbol{W}_t\boldsymbol{A}_t\right)\boldsymbol{x}^{(kT)} + \sum_{t=1}^{T-1}\left[\left(\prod_{s=T}^{t+1}(\boldsymbol{I} - \lambda_k \boldsymbol{V}^{-1}\boldsymbol{A}_s^{\mathrm{T}}\boldsymbol{W}_s\boldsymbol{A}_s)\right)\lambda_k \boldsymbol{V}^{-1}\boldsymbol{A}_t^{\mathrm{T}}\boldsymbol{W}_t\boldsymbol{b}_t + \lambda_k \boldsymbol{V}^{-1}\boldsymbol{A}_t^{\mathrm{T}}\boldsymbol{W}_t\boldsymbol{b}_t\right]. \tag{31}$$

Let $\lambda_k = 20.0$. After 20 cycles, the reconstructed images using three different block partition methods are shown in Fig 2. All the images are shown in displayed range $[0.95, 1.05]$. From left to right and from top to bottom: (a) real image, (b) reconstructed image with SeqBlock1, (c) reconstructed image with SeqBlock2, and (d) reconstructed image with QRBlock. Reconstruction results show that all block partition methods can provide proper reconstructed images.

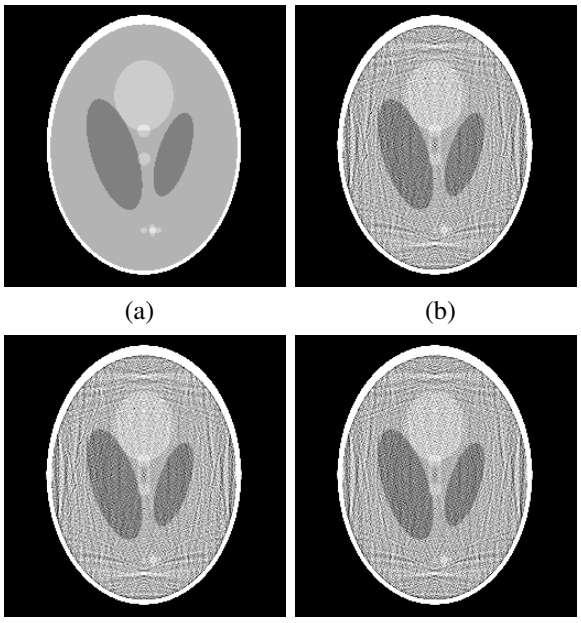

Fig 2. Results of the 20th iteration cycle using block traversal method

The RES and RMSE of different partition methods are listed in Table III. To more intuitively analyze the data, the changes of RES and RMSE with iteration cycles are also shown in Figs 3 and 4. The RES of the reconstruction algorithm decreases with the iteration cycles. However, the RMSE of reconstructed images decrease significantly at the beginning of iteration cycles, and increases slightly with the further increase of iteration cycles. According to Table III, if we use the same RES as the stopping criterion, the iteration cycle using QRBlock is less than the iteration cycles using SeqBlock1 and SeqBlock2, and the reconstructed image obtained by QRBlock has much smaller RMSE.

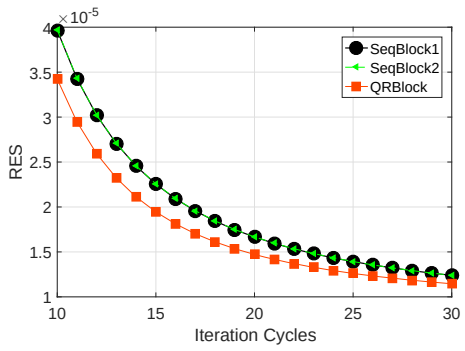

Fig 3. RES plotted against iteration cycles

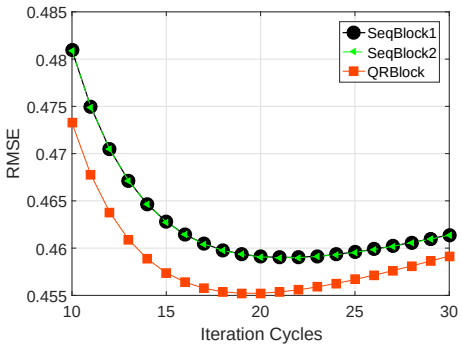

Fig 4. RMSE plotted against iteration cycles

C. Reconstruction with Random Order of Blocks

To observe the influence of the block order on the reconstruction results, random sorting and random selection methods are introduced to generate the serial number of the blocks used in iteration cycle.

- Random sorting: generate a random sequence of $\{1, 2, \ldots, T\}$, that means the order in which blocks are used is random.
- Random selection: randomly select an index from the set $\{1, 2, \ldots, T\}$ and repeat the selection for T times. Indices can be reused in one iteration cycle.

Following the block partition methods and parameter settings in previous subsection, we study the change of RMSE with iteration cycles. Considering the uncertainty of the random methods, the following data is derived from the mean of 10 groups of repeated experiments.

The mean and standard deviation of RMSE of two different random methods are listed in Table IV and Table V, respectively. And the mean of RMSE is also shown in Figs 5 and 6. From the tables and the figures, we find out that the RMSE of the iterative sequence generated by random QRBlock is better than that of SeqBlock1 and SeqBlock2. According to the standard deviation of the random experiments, RMSE is less affected by the order of QRBlock than that of SeqBlock1 and SeqBlock2. Next we compare the two different random method. The iteration sequence constructed by random sorting method not only converges faster than that constructed by random selection method, but also has smaller RMSE. One of the reasons is that during one iteration cycle, it is very likely that some blocks are not used and some blocks are reused for random selection method.

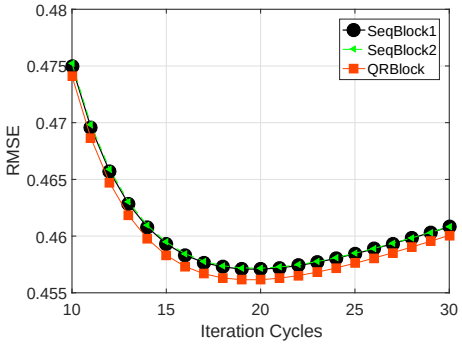

Fig 5. RMSE plotted against iteration cycles of random sorting methods

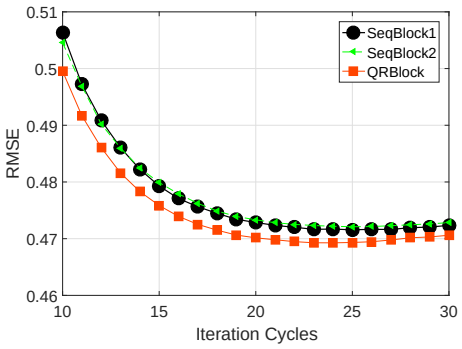

Fig 6. RMSE plotted against iteration cycles of random selection methods

D. Discussions on Numerical Tests

To make it clearer, we provide some remarks on the numerical experiments of block partition strategy and block iterative method.

- Two criteria, namely, weighted column correlation and weighted relative volume are used to construct the blocks. If the former criterion is adopted alone, the criterion only affects a small part of the row vectors of $\boldsymbol{A}$, and too many small blocks will be formed by those vectors. And if the latter criterion is adopted alone, it will lead to too few elements in some blocks. Therefore, the two need to be satisfied same.
- The block strategy we proposed is suitable for the imaging matrices. Multiple parts in iterative formula (31) can be calculated in advance if the blocks are determined, so that proper reconstructed image can be achieved faster.
- If the relaxation coefficient λ_k is set up to 100 or more, the RMSE decreases faster but meanwhile the images of different iteration cycles oscillate dramatically. It is not conducive to obtaining stable reconstructed images. According to known results of SART, the condition $\lambda_k \to 0$ guarantees the convergence of the sequence. Therefore, we propose using variable coefficients to obtain stable results in future tests.
- With the progress of the iteration, although the RES is still declining, the RMSE is gradually recovering step by step. Therefore, timely stopping of the iteration is of necessity in running the reconstruction algorithm.

V. Conclusion

In this paper, we propose a block partition strategy for the block Landweber scheme. Using thin oblique QR decomposition, we translate the analysis of the sub imaging matrix $\boldsymbol{A}_t$ into the analysis of the upper triangular matrix $\boldsymbol{R}_t$. We examine the hyper-parallel polyhedron represented by $\boldsymbol{R}_t$, and combine the relative volume criterion and the ratio of the maximum to minimum diagonal elements criterion to construct the block partition of imaging matrix $\boldsymbol{A}$. Then a follow-up sensitivity analysis is conducted. In order to solve the memory consumption problem of oblique QR decomposition, we also design pseudo code for updating the two criteria of block partition. Finally, in numerical tests, we apply our block partition strategy to X-ray CT imaging matrix $\boldsymbol{A}$, and use block SART to reconstruct the image. The numerical tests show that our block partition method

TABLE III
RES AND RMSE OF DIFFERENT BLOCK PARTITION METHODS

Iteration cycles	RES			RMSE		
	SeqBlock1	SeqBlocl2	QRBlock	SeqBlock1	SeqBlocl2	QRBlock
11	3.42691E-05	3.43069E-05	2.94580E-05	0.474944	0.474919	0.467769
12	3.01920E-05	3.02252E-05	2.59123E-05	0.470474	0.470447	0.463791
13	2.70350E-05	2.70644E-05	2.32111E-05	0.467131	0.467102	0.460910
14	2.45425E-05	2.45686E-05	2.11109E-05	0.464636	0.464606	0.458842
15	2.25405E-05	2.25638E-05	1.94480E-05	0.462786	0.462755	0.457384
16	2.09079E-05	2.09289E-05	1.81099E-05	0.461432	0.461400	0.456390
17	1.95586E-05	1.95774E-05	1.70174E-05	0.460462	0.460429	0.455749
18	1.84296E-05	1.84466E-05	1.61136E-05	0.459793	0.459759	0.455380
19	1.74747E-05	1.74901E-05	**1.53570E-05**	0.459359	0.459325	**0.455222**
20	1.66590E-05	1.66729E-05	1.47166E-05	0.459112	0.459077	0.455227
21	**1.59559E-05**	**1.59686E-05**	1.41692E-05	**0.459014**	**0.458979**	0.455359
22	1.53450E-05	1.53565E-05	1.36970E-05	0.459033	0.458998	0.455590
23	1.48102E-05	1.48207E-05	1.32863E-05	0.459147	0.459112	0.455899
24	1.43388E-05	1.43483E-05	1.29263E-05	0.459337	0.459301	0.456268
25	1.39206E-05	1.39294E-05	1.26086E-05	0.459587	0.459552	0.456683
26	1.35475E-05	1.35555E-05	1.23262E-05	0.459886	0.459850	0.457135
27	1.32128E-05	1.32202E-05	1.20738E-05	0.460223	0.460188	0.457614
28	1.29112E-05	1.29180E-05	1.18469E-05	0.460592	0.460557	0.458114
29	1.26380E-05	1.26442E-05	1.16418E-05	0.460985	0.460951	0.458630
30	1.23895E-05	1.23952E-05	1.14556E-05	0.461398	0.461364	0.459156

TABLE IV
MEAN AND STANDARD DEVIATION OF RMSE USING RANDOM SORTING

Iteration	SeqBlock1		SeqBlock2		QRBlock	
	mean	std	mean	std	mean	std
11	0.469595	1.16214E-03	0.469823	8.29025E-04	0.468653	6.53275E-04
12	0.465682	1.14355E-03	0.465885	8.02771E-04	0.464689	6.49087E-04
13	0.462833	1.12568E-03	0.463016	7.80029E-04	0.461817	6.44076E-04
14	0.460778	1.10838E-03	0.460942	7.59752E-04	0.459757	6.38521E-04
15	0.459321	1.09192E-03	0.459468	7.41554E-04	0.458305	6.32531E-04
16	0.458319	1.07600E-03	0.458450	7.25325E-04	0.457314	6.26061E-04
17	0.457664	1.06090E-03	0.457782	7.10412E-04	0.456676	6.19798E-04
18	0.457278	1.04645E-03	0.457384	6.96893E-04	0.456309	6.13111E-04
19	0.457100	1.03267E-03	0.457195	6.84308E-04	**0.456151**	**6.06845E-04**
20	**0.457084**	**1.01968E-03**	**0.457169**	**6.72390E-04**	0.456155	6.00391E-04
21	0.457195	1.00674E-03	0.457271	6.61442E-04	0.456287	5.94011E-04
22	0.457405	9.94895E-04	0.457472	6.50957E-04	0.456517	5.87853E-04
23	0.457693	9.83293E-04	0.457752	6.41235E-04	0.456824	5.81961E-04
24	0.458041	9.71954E-04	0.458093	6.32144E-04	0.457191	5.75792E-04
25	0.458436	9.61369E-04	0.458482	6.23250E-04	0.457605	5.70097E-04
26	0.458868	9.51107E-04	0.458908	6.15173E-04	0.458054	5.64400E-04
27	0.459328	9.41062E-04	0.459362	6.07224E-04	0.458531	5.58903E-04
28	0.459809	9.31619E-04	0.459838	5.99691E-04	0.459028	5.53577E-04
29	0.460306	9.22286E-04	0.460331	5.92438E-04	0.459541	5.48314E-04
30	0.460815	9.13599E-04	0.460835	5.85550E-04	0.460064	5.43238E-04

TABLE V
MEAN AND STANDARD DEVIATION OF RMSE USING RANDOM SELECTION

Iteration	SeqBlock1		SeqBlock2		QRBlock	
	mean	std	mean	std	mean	std
11	0.497201	4.49855E-03	0.496885	4.78216E-03	0.491668	2.04716E-03
12	0.490863	3.87034E-03	0.490211	4.67901E-03	0.486056	1.94324E-03
13	0.486039	3.18215E-03	0.485990	4.16539E-03	0.481578	1.84636E-03
14	0.482228	2.90154E-03	0.482421	3.75170E-03	0.478307	1.53615E-03
15	0.479284	2.60307E-03	0.479899	3.85578E-03	0.475846	1.38901E-03
16	0.477075	2.20408E-03	0.477902	3.48999E-03	0.473932	1.14902E-03
17	0.475638	2.15564E-03	0.476224	3.48478E-03	0.472521	1.10669E-03
18	0.474461	2.20548E-03	0.474880	3.42949E-03	0.471497	1.36817E-03
19	0.473412	2.15669E-03	0.473910	3.44566E-03	0.470635	1.22799E-03
20	0.472857	2.26411E-03	0.473330	3.30741E-03	0.470150	1.22144E-03
21	0.472347	2.17319E-03	0.472815	3.22079E-03	0.469811	1.31117E-03
22	0.472008	2.11292E-03	0.472524	3.19330E-03	0.469478	1.32197E-03
23	0.471659	1.95085E-03	0.472324	3.11777E-03	0.469278	1.36146E-03
24	0.471686	2.00967E-03	0.472180	3.06352E-03	**0.469267**	**1.20274E-03**
25	**0.471571**	**1.88960E-03**	**0.472109**	**2.98274E-03**	0.469331	1.28729E-03
26	0.471643	1.75472E-03	0.472134	2.99456E-03	0.469461	1.25532E-03
27	0.471633	1.64003E-03	0.472292	2.82730E-03	0.469771	1.27374E-03
28	0.471934	1.66084E-03	0.472448	2.87689E-03	0.470159	1.20503E-03
29	0.472046	1.61957E-03	0.472610	2.84246E-03	0.470305	1.27871E-03
30	0.472348	1.69673E-03	0.472830	2.91351E-03	0.470607	1.12123E-03

can provide better reconstructed images with fewer iteration cycles when compared with sequential block partition under the same stopping rule of RES.

ACKNOWLEDGMENT

The author would like to thank Professor Huidan Liu (College of Foreign Languages, Shanghai Maritime University) for her advice on English writing.

REFERENCES

[1] S. Kaczmarz, "Approximate solution of systems of linear equations," *International Journal of Control*, vol. 57, no. 6, pp. 1269–1271, 1993.

[2] T. Strohmer and R. Vershynin, "A randomized Kaczmarz algorithm with exponential convergence," *Journal of Fourier Analysis and Applications*, vol. 15, no. 2, pp. 262–278, 2009.

[3] A. Zhdanov, "The method of augmented regularized normal equations," *Computational Mathematics and Mathematical Physics*, vol. 52, no. 2, pp. 194–197, 2012.

[4] Z. Bai and W. Wu, "On relaxed greedy randomized Kaczmarz methods for solving large sparse linear systems," *Applied Mathematics Letters*, vol. 83, no. 3, pp. 21–26, 2018.

[5] ——, "On greedy randomized Kaczmarz method for solving large sparse linear systems," *SIAM Journal on Scientific Computing*, vol. 40, no. 1, pp. A592–A606, 2018.

[6] X. Jiang, K. Zhang, and J. Yin, "Randomized block Kaczmarz methods with k-means clustering for solving large linear systems," *Journal of Computational and Applied Mathematics*, vol. 403, no. 113828, pp. 1–14, 2022.

[7] A. Li, "Preconditioned SSOR iterative method for linear system with M-matrices," *Lecture Notes in Engineering and Computer Science: Proceedings of The World Congress on Engineering and Computer Science 2010, WCECS 2010, 20-22 October, 2010, San Francisco, USA*, pp. 155–158.

[8] O. Kardani, A. V. Lyamin, and K. Krabbenhoft, "Iterative solution of large sparse linear systems arising from application of interior point method in computational geomechanics," *Lecture Notes in Engineering and Computer Science: Proceedings of The World Congress on Engineering 2013, WCE 2013, 3-5 July, 2013, London, U.K.*, pp. 216–221.

[9] M. Lan, J. Xu, and W. Gao, "A class of nonstationary upper and lower triangular splitting iteration methods for ill-posed inverse problems," *IAENG International Journal of Computer Science*, vol. 47, no. 1, pp. 118–129, 2020.

[10] M. Jiang and G. Wang, "Convergence studies on iterative algorithms for image reconstruction," *IEEE Transactions on Medical Imaging*, vol. 22, no. 5, pp. 569–579, 2003.

[11] A. Andersen and A. Kak, "Simultaneous algebraic reconstruction technique (SART): A superior implementation of the ART algorithm," *Ultrasonic Imaging*, vol. 6, no. 1, pp. 81–94, 1984.

[12] G. Cimmino, "Calcolo approssimato per le soluzioni del sistemi di equazioni lineari," *La Riserca Scientifica*, vol. 16, no. 2, pp. 326–333, 1938.

[13] Y. Censor, D. Gordon, and R. Gordon, "Component averaging: An efficient iterative parallel algorithm for large and sparse unstructured problems," *Parallel Computing*, vol. 27, no. 6, pp. 777–808, 2001.

[14] Y. Censor and T. Elfving, "Block-Iterative algorithms with diagonally scaled oblique projections for the linear feasibility problem," *SIAM Journal on Matrix Analysis and Applications*, vol. 24, no. 1, pp. 40–58, 2002.

[15] J. Wang and Y. Zheng, "On the convergence of generalized simultaneous iterative reconstruction algorithms," *IEEE Transactions on Image Processing*, vol. 16, no. 1, pp. 1–6, 2007.

[16] G. Qu, C. Wang, and M. Jiang, "Necessary and sufficient convergence conditions for algebraic image reconstruction algorithms," *IEEE Transactions on Image Processing*, vol. 18, no. 2, pp. 435–440, 2009.

[17] G. Han, G. Qu, and M. Jiang, "Relaxation strategy for the Landweber method," *Signal Processing*, vol. 125, no. 8, pp. 87–96, 2016.

[18] T. Elfving and T. Nikazad, "Stopping rules for Landweber-type iteration," *Inverse Problems*, vol. 23, no. 4, pp. 1417–1417, 2007.

[19] A. Kirsch, *An introduction to the mathematical theory of inverse problems*. Cham, Switzerland: Springer, 2021.

[20] C. Wang and T. Zhou, "The order of convergence for Landweber scheme with alpha,beta-rule," *Inverse Problems and Imaging*, vol. 6, no. 1, pp. 133–146, 2012.

[21] J. Qiu and M. Xu, "A method of symmetric block-iterative for image reconstruction," *Journal of Electronics and Information Technology*, vol. 29, no. 10, pp. 2296–2300, 2007.

[22] J. Sun, "Studies of the relaxation parameter selection of the block-iterative algorithm for image reconstruction," *Computerized Tomography Theory and Applications*, vol. 16, no. 2, pp. 14–19, 2007.

[23] P. Hansen and M. Saxild-Hansen, "AIR Tools: A MATLAB package of algebraic iterative reconstruction methods," *Journal of Computational and Applied Mathematics*, vol. 236, no. 8, pp. 2167–2178, 2012.

[24] G. Han, G. Qu, and Q. Wang, "Weighting algorithm and relaxation strategies of the Landweber method for image reconstruction," *Mathematical Problems in Engineering*, vol. 2018, no. 9, pp. 1–19, 2018.

[25] Y. Zhang, Y. Yang, and W. Lu, "Block-iterative algorithm with row projection for consistent linear system," *Journal of Nanjing Normal University (Engineering and Technology)*, vol. 6, no. 1, pp. 47–51, 2006.

[26] Y. Censor, "Parallel application of block-iterative methods in medical imaging and radiation therapy," *Mathematical Programming*, vol. 42, no. 1, pp. 307–325, 1988.

[27] Y. Censor and G. Herman, "Block-iterative algorithms with underrelaxed Bregman projection," *SIAM Journal on Optimization*, vol. 13, no. 1, pp. 283–297, 2002.

[28] J. Liu, X. Lu, and X. Cao, "Diagnosis of the second type of ill-conditioning based on QR decomposition," *Science of Surveying and Mapping*, vol. 36, no. 4, pp. 92–94, 2011.